International Journal of Nanomedicine

Dovepress
Taylor & Francis Group

Open Access Full Text Article

ORIGINAL RESEARCH

Tolvaptan-Loaded Tomato-Derived Nanovesicles: Characterization and Evaluation of Cytotoxicity, Wound Healing Potential and the Effects on Cyst Formation in Renal Cell Lines

Ramila Mammadova[1,2,*], Feby Wijaya Pratiwi[2,3,*], Immacolata Fiume[1], Eslam Abdelrady[2], Olha Makieieva[2], Laura Zucaro[4], Francesco Trepiccione[4], Seppo Vainio[2,3,*], Gabriella Pocsfalvi[1,*]

[1]National Research Council of Italy, Institute of Biosciences and BioResources, Naples, Italy; [2]Faculty of Biochemistry and Molecular Medicine, University of Oulu, Oulu, Finland; [3]Kvantum Institute, University of Oulu, Oulu, Finland; [4]Department of Translational Medical Sciences, University of Campania Luigi Vanvitelli, Naples, Italy

*These authors contributed equally to this work

Correspondence: Gabriella Pocsfalvi, National Research Council of Italy, Institute of Biosciences and BioResources, via P. Castellino, 111, Naples, 80131, Italy, Email gabriellakatalin.pocsfalvi@cnr.it

Purpose: Plant-derived nanovesicles (PDNVs) are promising candidates for next-generation drug delivery system due to their scalability, low cytotoxicity and immunogenicity, and efficient cellular uptake. Here, tomato fruit-derived PDNVs were loaded with tolvaptan, a vasopressin V2-receptor antagonist with the aim to reduce drug cytotoxicity, control drug release and to improve drug efficiency in vitro.

Methods: Tolvaptan was encapsulated by extrusion and electroporation. Entrapment efficiency (EE%) and drug loading capacity (DLC%) were optimized by changing the drug-to-PDNV ratio and time-dependent drug release rate was evaluated at two different pH. Tolvaptan-loaded PDNVs were characterized using physiochemical and morphological methods. Cellular uptake of fluorescently labelled tolvaptan-loaded PDNVs was evaluated. The cytotoxicity and effects of tolvaptan-loaded PDNVs on cyst formation and cell migration were studied in different renal cell cultures.

Results: Electroporation resulted in higher EE% and DLC% than extrusion for the encapsulation of tolvaptan into PDNVs. MDCK cells efficiently uptake tolvaptan-loaded PDNVs. The release of the tolvaptan was time and pH dependent. Enhanced cell proliferation, suppressed cyst growth, and altered cyst morphology compared with controls was observed. Migration assay demonstrated that tolvaptan-encapsulated PDNVs had a favourable effect on enhancing wound healing and cell migration in renal cells.

Conclusion: Tolvaptan-loaded PDNVs show promising features as a natural next-generation nanoscale delivery system in vitro for time and pH-dependent release of hydrophobic drugs, such as tolvaptan.

Keywords: plant-derived nanovesicles, drug delivery, tomato, tolvaptan, polycystic kidney disease

Introduction

In the fields of biotechnology and pharmaceutical research, the confluence of new drug delivery strategies and natural substances has opened up possibilities for new therapeutic interventions.[1,2] Natural nano-drug delivery systems are increasingly being investigated as promising solutions to overcome the barriers faced in clinical applications. Amongst these, nanometer-sized, biomembrane enclosed plant-derived vesicles have emerged recently due to their intrinsic characteristic to transport complex bioactive cargoes including proteins, lipids, and nucleic acids.[3] Here, we use "plant-derived nanovesicles" (PDNVs) as an umbrella term for the kind of nanomaterial obtained from homogenized whole plants, plant tissues or organs. PDNVs are isolated from homogenized and therefore highly complex materials using

Received: 1 October 2024
Accepted: 3 January 2025
Published: 17 May 2025

methods commonly applied in extracellular vesicle (EV) research, such as ultracentrifugation, size-exclusion chromatography, and tangential flow filtration. Pristine PDNVs contain a highly complex mixture of intracellular and extracellular transporter vesicles as well as vesicles formed during the isolation process. These nanomaterials hold promise as natural nano-drug delivery systems because of their biocompatibility, low immunogenicity, and ability to navigate biological barriers.[4–6] Moreover, the production of PDNVs is easily scalable.

PDNVs have been isolated from various plants, such as ginger,[7–10] grapefruit,[11–13] kiwi,[14] cucumber,[6] cabbage,[15] asparagus,[16] and tomato,[17] just to mention some. They could be sustainable alternatives to mammalian EVs with the potential for large-scale production, thus advancing prospects for novel drug delivery interventions. Several PDNVs have been loaded with different natural or synthetic molecules and have been studied for their potential to deliver exogenous ingredients in vitro and in vivo. For example, grapefruit PDNVs were loaded with curcumin and doxorubicin to alleviate inflammation and inhibit tumor growth, respectively, in a DSS-induced mouse colitis model.[11] In other studies, grapefruit PDNVs loaded with therapeutic microRNAs were used to target brain cancer[12] or liver metastasis of colon cancer.[13] Finally, kiwifruit PDNVs were also exploited for the delivery of sorafenib, a protein kinase inhibitor drug to target hepatocellular carcinoma cells (HCC).[14] PDNVs could be useful as cell-free therapy for several diseases. Drug-delivery applications of PDNVs isolated from different sources have been recently reviewed.[18] There are several potential advantages of using PDNVs as nanocarrier of various drugs for the treatment of diseases. These include their natural green origin, the opportunity to isolate them in a high yield from economical plant resources, biocompatibility, biodegradability, and stability within the gastrointestinal tract.

We previously isolated micro- and nano-sized PDNVs from tomatoes using differential ultracentrifugation (dUC), and subsequently applied size-exclusion chromatography (SEC) or density gradient ultracentrifugation (DGUC) purification methods to obtain distinct PDNVs populations.[17,19] These tomato-derived PDNVs have been shown to possess intrinsic anti-inflammatory activity, which was further increased by encapsulation of the exogenous natural compound curcumin.[20] Indeed, the low-density DGUC fraction of tomato PDNVs was shown to downregulate the production of IL-1β at the mRNA level in a model of LPS-induced inflammation in the THP-1 human monocytic cell line, and a proteomic analysis of this PDNVs subpopulation revealed several inflammatory modulators as part of the protein constituents.

Here, by building on the intrinsic anti-inflammatory and carrier properties of tomato-derived PDNVs, we aimed to supplement them with antiproliferative activity by encapsulating a synthetic drug, tolvaptan. Tolvaptan is a vasopressin antagonist selective for the V2-subtype vasopressin receptor (V2R)[21] and can act as an antagonist chaperone for the mutated V2R receptor, showing high selectivity for V2R.[22] Recently, tolvaptan was shown to arrest renal cyst growth in autosomal dominant polycystic kidney disease (ADPKD)[23–26] and cellular proliferation in cultured renal cancer cells.[27]

Clinical trials, such as TEMPO 3:4 (NCT00428948) and the Replicating Evidence of Preserved Renal Function: an Investigation of Tolvaptan Safety and Efficacy in ADPKD (REPRISE) trial (NCT02160145) have demonstrated that tolvaptan treatment was effective in decreasing renal volume growth, declining the estimated glomerular filtration rate (GFR), and maintaining renal function in patients with ADPKD.[25,28] It has also efficacy on the patients who are at the risk of renal failure or with quickly progressive ADPKD.[29] However, tolvaptan has potential side effects too. For instance, increased thirst and urination are the frequently observed adverse reactions, coming from the diuretic impact of tolvaptan.[11] Besides, some patients may also experience electrolyte imbalances,[29] particularly elevated sodium levels (hypernatremia), caused by increased water excretion,[30] liver enzyme abnormalities,[30] nausea, or diarrhea.[30] Therefore, tolvaptan treatment requires careful monitoring by healthcare providers, and some modifications might be required to control adverse reactions.

Tolvaptan exhibits low solubility (50 ng/mL at 25 °C, pH 2–12), low permeability, and low bioavailability. To enhance oral bioavailability, methods to improve solubility, dissolution rate, and permeability have been employed, including liposomes,[31] nanosuspensions,[31] solid dispersions,[31] and self-emulsifying formulations.[31] To improve water solubility and enable intravenous use Tolvaptan, Fujiki et al synthetized tolvaptan sodium phosphate (OPC-61815) as a pro-drug of tolvaptan that was evaluated in a pharmacokinetics study.[32] Lee et al addressed this issue by optimizing a self-microemulsifying drug delivery system through a design of the experiment (DoE) approach.[31] Employment of oils, surfactants, and cosurfactants like Capryol® 90, Tween 20, and Transcutol® HP, increased self-emulsification efficiency

in the formulation that resulted in an increased tolvaptan bioavailability. Targeting tolvaptan delivery to specific sites remains challenging. One possible option could be the use of plant-derived nanovesicles for their encapsulation. PDNVs have been demonstrated to possess unique advantages in the fabrication of nanocarriers for drug delivery.[3]

In this study, we employed two loading methods to encapsulate tolvaptan: extrusion and electroporation. The physical and morphological characteristics and impact of tolvaptan-loaded tomato PDNVs on the regulation of cell proliferation, cytotoxicity, uptake, cell migration, and cystogenesis were studied using different kidney cell lines each mimicking different aspects of kidney-related conditions. Ureteric bud (UB) cells are useful for modeling nephrogenesis, and Madin-Darby canine kidney (MDCK) cell is a commonly used cell line that retains many characteristics of the distal nephron and used for in vitro cystogenesis studies. Moreover, two of the cell lines were cancer cell lines, Renca and Caki-1. Renca is an epithelial cell line that was isolated from the kidney of a male mouse with renal cortical adenocarcinoma while Caki-1 cells, representing renal carcinoma and cell migration models.

Materials and Methods

Isolation of PDNVs from Tomato Fruit and Loading Them with Tolvaptan

Tomato (*Solanum lycopersicum* L., 1753) Piccadilly plump tomatoes were from commercial source from Real Frutta S.r. l., Napoli, Italy. PDNVs were isolated using dUC as described by Bokka et al.[17] Tolvaptan was obtained from MedChemExpress (Sollentuna, Sweden). Tolvaptan was encapsulated in PDNVs using two methods: extrusion and electroporation.

Preparation of Tolvaptan-Loaded Tomato PDNVs by Extrusion

Tomato PDNVs (5 mg protein) were vacuum-dried (Speed Vac, SC100, Savant Instruments, Inc. Farmingdale, NY, USA), re-suspended in 1 mL of methanol, and transferred to a round-bottom glass vial. Tolvaptan (0.5 mg) dissolved in methanol (1 mg/mL) was added to the PDNVs sample (PDNVs:tolvaptan ratio 1:0.1), and the solvent was evaporated slowly under a nitrogen stream. The dried sample was rehydrated in extraction buffer (filtered using 0.02 μm Whatman® Anotop® syringe filter) at 65 °C overnight. The sample was centrifuged at 500 × g for 5 min, the supernatant was filtered through a 0.22 μm syringe filter (Whatman®), and then extruded using an Avanti mini extruder (Avanti Polar Lipids Inc., Alabama, USA) 42 extrusion cycles with two different polycarbonate membranes, 0.2 μm and 0.1 μm pores. The extruded sample was re-purified by UC at 100,000 × g for 2 h at 4 °C using an SW55Ti rotor.

Preparation of Tolvaptan-Loaded Tomato PDNVs by Electroporation

Electroporation was performed at two different PDNVs to tolvaptan ratios 1:1 and 10:1 keeping the tolvaptan quantity fixed at 0.5 mg and using either 0.5 mg or 5 mg PDNVs. PDNVs (protein concentration 4.2 mg/mL) and tolvaptan (1 mg/mL solution in methanol) were mixed in a 2 mL Eppendorf tube. After overnight incubation at room temperature, the sample was transferred to an Eppendorf tube and diluted with Resuspension Buffer R (Neon™ Electroporation System, Invitrogen, Carlsbad, CA, USA) at a 1:1 ratio. The diluted mixture (100 μL) was carefully loaded into a Neon pipette. Electroporation was performed by applying a voltage of 750 V, with a pulse width of 15 ms and five pulses. The electroporated sample was repurified in a 2 mL Quick-Seal polyallomer tube by UC at 100,000 × g for 3 h at 4 °C using a TLA 120.2 rotor, Beckman Optima TL ultracentrifuge).

After loading, the protein concentrations of the samples were determined using a Qubit Protein Assay (Thermo Fisher Scientific, Rockford, IL, USA) according to the manufacturer's instructions. Tolvaptan concentrations were determined using UV-Vis spectrophotometry based on the absorbance measured at 269 nm.

Determination of Entrapment Efficiency (EE%) and Drug Loading Capacity (DLC%)

The entrapment efficiency (EE%) and drug loading capacity (DLC%) of tolvaptan loading into the PDNVs were calculated according to the following equations:[20]

EE (%)=(amount of the encapsulated tolvaptan)/(initial amount of tolvaptan added)×100%

DLC (%)=(amount of the encapsulated tolvaptan)/(total amount of the PDNVs carrier)×100%

The amount of the PDNVs is expressed in protein quantity.

 https://doi.org/10.2147/IJN.S498012

Drug Release Assay of Tolvaptan-Loaded PDNVs

The release of tolvaptan from nanovesicles was carried out under two conditions, PBS solution pH 7.4, and tris-HCL solution pH 5.0. 300 µL of tolvaptan-loaded NVs containing 350 µg protein and 39 µg tolvaptan were loaded onto the polyethersulfone (PES) membrane of Spin-X® UF concentrator tube (100 kDa cutoff pore size, Corning, UK) with 5 mL of PBS/tris-HCL solution, and stirred at room temperature. At each predetermined time point, 200 µL of sample was collected from the release medium and the equal volume of buffer solution was added. The amount of tolvaptan in collected samples was determined by UV-Vis spectroscopy by measuring the absorbance at 269 nm. The drug release rate of tolvaptan was calculated according to the formula:

Drug release % = Amount of the released drug/Amount of the added drug × 100%

Characterization of Tomato Nanovesicles

Nanoparticle Tracking Analysis (NTA)

The nanoparticle concentration and size of both pristine tomato PDNVs and the drug-loaded tomato PDNVs were assessed using nanoparticle-tracking analysis (NTA) on a NanoSight NS300 instrument (Malvern Panalytical, Malvern, UK). Each sample, comprising 2 µg of PDNVs (expressed as protein quantity), was diluted to a volume of 1 mL with Milli-Q water, and 1 mL of the diluted sample was introduced into the instrument. The analysis was conducted with a camera level set at 14 and detection threshold at level 3. Subsequently, the acquired data were processed and examined using the NTA software version 3.4.

Zeta Potential Measurements

The zeta potentials of both the pristine and drug-loaded PDNVs were determined using a Zetasizer Nano ZS instrument (Malvern Instruments Ltd., Malvern, UK), incorporating a laser source with a wavelength of 633 nm and a scattered angle of 13°. The instrument was calibrated according to the manufacturer's instructions by measuring the known surface charge (40 ± 5.8mV) of 100 nm polystyrene nanoparticles. Each sample, consisting of 2 µg of PDNVs (expressed as protein quantity), was diluted to 1 mL in MilliQ water and 800 µL of the diluted sample was introduced into folded capillary cell cuvettes of type DTS 1070 (Malvern Instruments Ltd., Malvern, UK). The zeta potentials of the samples were measured three times at 25 °C, employing an automatic number of runs and voltage selection with an equilibration time of 120 s.

Transmission Electron Microscopy (TEM)

Transmission electron microscopy (TEM) imaging with a Tecnai G2 Spirit instrument (FEI, Eindhoven, The Netherlands) was used to visualize the surface morphology of both the pristine and drug-loaded PDNVs. Briefly, 2 µL of each sample was applied to a Formvar carbon-coated grid that had been glow-discharged. Subsequently, negative staining was carried out using 2% uranyl acetate, and the samples were examined using a Tecnai G2 Spirit transmission electron microscope (FEI, Eindhoven, The Netherlands). Images were captured at a magnification of 1:23000 using a charge-coupled device camera (Quemesa; Olympus Soft Imaging Solutions GMBH, Münster, Germany).

Cell Lines

The mouse Renca (American Type Culture Collection (ATCC) CRL-2947™) epithelial cell line derived from a spontaneous renal cortical adenocarcinoma in BALB/cCr mice; Caki-1 (ATCC HTB-46™) human renal cell carcinoma cell line and Madin-Darby canine kidney (MDCK, NBL-2, ATCC CCL-34™) were obtained from American Type Culture Collection (ATCC). The ureteric bud (UB) immortalized cell line[33] was gifted by Barasch's lab (Columbia University, USA). The MDCK, UB, and Renca cells were cultured in Dulbecco's modified Eagle's medium (DMEM) supplemented with 10% of fetal bovine serum (FBS) and 1% of penicillin. Caki-1 cells were cultured in Eagle's Minimum Essential Medium (EMEM) with 10% FBS). Cells were grown at 37 °C and 5% CO_2.

Cytotoxicity and Cell Proliferation Assays

An IncuCyte Cell Count Proliferation Assay was used to measure the cytotoxicity, cell viability, and proliferation of the pristine and drug-loaded PDNVs. The cells were detached by application of a proteolytic enzyme, trypsin, and

centrifuged at 125 × *g* for 5 min, counted by TC20™ Automatic Cell Counter (Bio-Rad), resuspended at 1×10^5 cells/mL concentration in DMEM supplemented with 10% FBS, 100 µL volumes were seeded into a 96-well flat bottom plate and incubated at 37 °C, 5% CO_2 overnight. After overnight incubation, the medium was removed, and the cells were washed with phosphate-buffered saline (PBS) and replaced with fresh medium containing tomato PDNVs samples. SYTOX Green high-affinity nucleic acid stain (diluted with medium 1:10000) was used to label the dying cells. Scanning was performed every 3 h at 10 × magnification, with a standard scan used to observe cell death over time. Dying cells were automatically quantified using IncuCyte image analysis tools. All samples were plated in triplicate.

Uptake of Tomato PDNVs by MDCK Cells

MDCK cells were seeded on a 12 well plate in a glass slide at a density of 2×10^5 cells/well. Cells were treated with 10 µg (1 mL/well, at the concentration of 0.01 µg/µL) of tomato PDNVs labelled with green fluorescent dye $DiOC_{18}$ and incubated for 1, 8, and 24 h at 37 °C. Then The cells were washed with PBS and fixed with 4% paraformaldehyde (PFA) solution at 4 °C overnight. PFA was then removed, and the cells were washed with PBS. Cell nuclei were stained with 4′,6-diamidino-2-phenylindole (DAPI) (Thermo Fisher Scientific, 62248, USA), and LysoTracker Deep Red (Invitrogen, L12492, USA) was used to stain lysosomes in MDCK cells. The results were visualized using a Leica Stellaris 8 DIVE confocal and multiphoton microscope (Leica Microsystems GmbH, Germany).

Flow Cytometry Analysis of Cellular Uptake

Quantitative cellular uptake of tolvaptan-loaded tomato PDNVs by MDCK cells was evaluated using flow cytometry. MDCK cells were seeded in a 6 well plate at a density of 1.55×10^5 cells/well, and cultured for 24 h. Cells were further treated with 20 µg of tomato PDNVs labelled with green fluorescent dye $DiOC_{18}$ (2 mL/well, at the concentration of 0.01 µg/µL) and incubated for 1, 8, and 24 h at 37 °C. After incubation the medium was removed, cells were washed with cold PBS twice, detached by trypsin, centrifuged at 300 × g for 3 min at 4 °C, resuspended in 300 µL of PBS, and analyzed by a flow cytometer (BD FACS symphony A5 SE, BD Biosciences, San Jose, CA, USA). The obtained data were analyzed using FlowJo software (version 10.10.0, FlowJo LLC).

In vitro Cyst Formation of MDCK Cells

For the cyst morphogenesis experiments, hESC-Qualified LDEV-Free Matrigel matrix (354277, Corning, NY, USA) was thawed overnight in a 4 °C refrigerator before use. About 200 µL of Matrigel matrix (10 mg/mL) was transferred into each well of a pre-chilled 24-well plate on the top of a glass coverslip, spread evenly with a pipette tip, and then incubated at 37 °C for 30 min to allow the Matrigel matrix to form a gel. MDCK cells were washed once with PBS, detached using trypsin to obtain a single-cell suspension, and pelleted by centrifugation at 125 × g for 5 min at room temperature. The cells were resuspended in MDCK complete medium (DMEM supplemented with 10% FBS) to adjust the final cell density to 3×10^5 cells/mL. About 250 µL volumes of cell suspension were added to each well of a precoated 24-well plate and then incubated at 37 °C for 30 min. The MDCK complete medium was chilled on ice and added Matrigel matrix to 10% of the final volume (final concentration: 0.8 to 1.1 mg/mL). Matrigel matrix medium (250 µL) was gently added to the plated culture. The cells were continuously cultured for eight days, and the Matrigel matrix medium mixture was changed every two days. Images were obtained using a Leica Stellaris 8 DIVE confocal and multiphoton microscope (Leica Microsystems GmbH, Germany).

Cell Migration Assay

An Incucyte ZOOM® 96-well scratch wound migration assay was performed to measure the basic cell migration parameters in vitro. Caki-1, MDCK, UB, and Renca cells were seeded at a density of 5×10^5 cells/well in an Incucyte ImageLock™ 96-well plate and incubated for 48 h. Once the cells reached 100% confluence, the culture medium was removed, replaced with serum-free medium containing 0.1% (w/v) metamycin, kept for 6 h at 37 °C in 5% CO_2 before making the scratching. Wounds were created using WoundMaker™ (Essen Biosciences, San Jose, CA, USA), a 96-pin mechanical device designed to create 700–800 µm wide homogeneous wounds in cell monolayers on 96-well ImageLock™ microplates. After creating wounds, the medium was removed, the cells were washed with PBS, and serum-free medium containing PDNVs samples (5 µg of PDNVs based on protein content and 0.25/2.9 µg of tolvaptan)

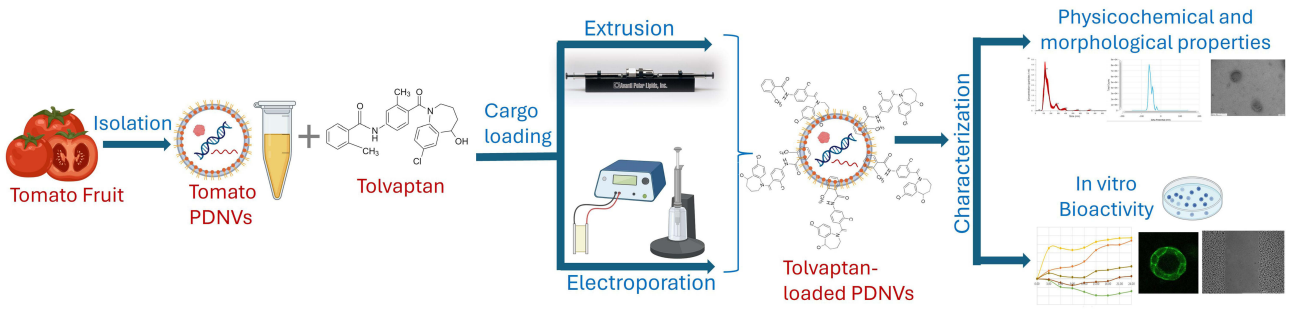

Figure 1 Schematic workflow of the isolation of tomato PDNVs, loading with tolvaptan and physiochemical, morphological and biological characterization (Figure was created by using Biorender[34]).

was added into the wells. The area that remained clear of cells was quantified for 48 h using an Incucyte S3 live analysis system (Essen Biosciences). Digital images were obtained every 2 h. Assays were performed in triplicate.

Statistical Analysis

The experiments were conducted in triplicate unless stated otherwise, with results presented as mean values accompanied by standard deviations. Statistical analysis was carried out using one-way ANOVA followed by Tukey's post-hoc test, utilizing OriginPro® 2022 (US). A p-value of less than 0.05 was considered statistically significant.

Results

Evaluation of Tolvaptan Loading into Tomato PDNVs and Characterization of Tolvaptan-Loaded PDNVs

PDNVs were isolated from the Piccadilly variant of tomatoes by dUC method as described previously.[17] The procedural workflow employed for the isolation, drug loading, and characterization of drug-loaded tomato PDNVs is summarized in Figure 1.

Two different methods, electroporation and extrusion, were evaluated for loading tolvaptan into the tomato PDNVs. To avoid unloaded tolvaptan and debris in the final sample, PDNVs were repurified after loading using ultracentrifugation. The final nanoparticle, protein, and tolvaptan concentrations were determined, and the entrapment efficiency (EE%) and drug loading capacity (DLC%) were calculated. Comparing the two methods, we observed slightly higher EE% and DLC% and particle concentration with electroporation (Table 1). Therefore, electroporation was used to optimize the loading at two different PDNVs to drug ratios. Keeping the initial tolvaptan quantity fixed at 0.5 mg, two PDNVs to tolvaptan ratios were attempted by increasing the PDNVs quantities 10 times from a ratio of 1:1 to 10:1. Almost 10 times more tolvaptan could be incorporated at a 1:1 ratio (2.9 µg) compared to a 10:1 ratio (0.3 µg). The EE% increased

Table 1 Encapsulation of Tolvaptan Into Tomato PDNVs Using Extrusion and Electroporation Methods, Entrapment Efficiency (EE%) and Drug Loading Capacity (DLC%). PDNVs Quantity Is Expressed in the Measured Protein Quantity. Particle Concentrations Were Measured by NTA and Expressed as Particle Numbers in mL of Final Sample

Loading	Initial PDNVs / Tolvaptan Ratio	Final PDNVs / Tolvaptan Ratio	Particles / mL in Final Sample	EE (%)	DLC (%)
Electroporation	1:1	1:0.5	$2.86 \times 10^{11} \pm 2.39 \times 10^{10}$	45	37
Electroporation	10:1	1:0.06	$4.42 \times 10^{11} \pm 3.21 \times 10^{10}$	16	6
Extrusion	10:1	1:0.05	$7.93 \times 10^{10} \pm 5.2 \times 10^{9}$	12	5

Abbreviations: PDNVs, plant-derived vesicles; EVs, extracellular vesicles; HCC, hepatocellular carcinoma cells; dUC, differential ultracentrifugation; SEC, size exclusion chromatography; DGUC, density gradient ultracentrifugation; V2R, vasopressin receptor; ADPKD, autosomal dominant polycystic kidney disease; EE%, entrapment efficiency; DLC%, drug loading capacity; NTA, Nanoparticle Tracking Analysis; TEM, Transmission electron microscopy; UB, ureteric bud; MDCK, Madin-Darby canine kidney; DMEM, Dulbecco's modified Eagle's medium; FBS, fetal bovine serum; EMEM, Eagle's Minimum Essential Medium; PFA, paraformaldehyde; DAPI, 4′,6-diamidino-2-phenylindole; PBS, phosphate buffered saline.

considerably from 16 to 45 and DLC% from 6 to 37 (Table 1). Consequently, PDNVs electroporated at a 1:1 ratio with tolvaptan were used in the in vitro experiments.

To characterize the PDNVs before and after loading with tolvaptan, the protein and particle concentrations, particle sizes, and zeta potentials were determined. Tomato fruit-derived pristine PDNVs had a mean diameter of 224.1 ± 12.6 nm, negative zeta potential of –55.03 mV, and contained 1.96×10^{11} ± 2.6×10^{10} particles/mL (9.8 x10^{10} ± 2.6×10^{7} particles/µg). After extrusion, we observed a reduction in diameter of the PDNVs (177.0 ± 9.7 nm), a lowered zeta potential of –62.45 mV, and a lowered particle number of 7.93×10^{10} ± 5.2×10^{9} /mL. These results suggest some loss and resizing the vesicles upon extrusion, as expected. Electroporation, similar to extrusion, slightly reduced the size (191.3 ± 6.3 nm) and zeta potential (–51.81 mV) of the vesicles but resulted in more particles numbers (2.86 x 10^{11} ± 2.39×10^{10} particles/mL) than extrusion.

Morphological Studies

The morphologies of the pristine and tolvaptan-loaded tomato PDNVs were analyzed by transmission electron microscopy (TEM). Transmission electron microscopy (TEM) revealed spherical lipid bilayer structures (Figure 2). While the vesicular structure was maintained upon loading, NTA results showed that the size of the tolvaptan-loaded PDNVs slightly decreased. Moreover, some aggregation was observed in the extrusion-prepared samples. The higher grade of aggregation can be attributed to the increased negative zeta potential of the particles.

However, we observed the preservation of the overall morphology and physical properties in both loading procedures, which highlights the resilient nature of tomato PDNVs as a drug delivery platform.

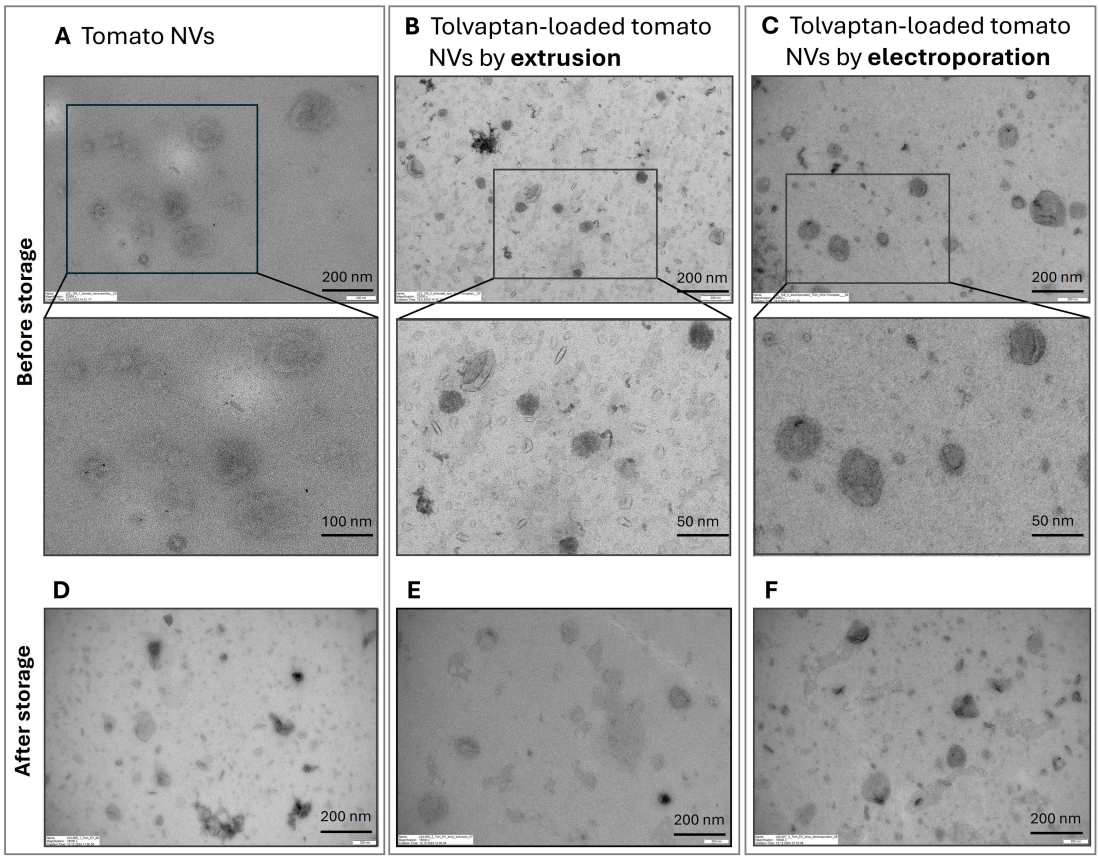

Figure 2 Representative transmission electron microscopy (TEM) images of (**A**) pristine tomato nanovesicles (NVs). (**B**) tolvaptan-loaded tomato NVs by extrusion. (**C**) tolvaptan-loaded tomato NVs by electroporation. (**D**) pristine tomato nanovesicles (NVs) after 1 year under − 80 °C storage conditions. (**E**) tolvaptan-loaded tomato NVs by extrusion after 1 year under − 80 °C storage conditions. (**F**) tolvaptan-loaded tomato NVs by electroporation after 6 months under − 80 °C storage conditions.

https://doi.org/10.2147/IJN.S498012

Stability of Tolvaptan-Loaded Tomato PDNVs

To study the stability of pristine and tolvaptan-loaded tomato-derived PDNVs, their protein concentration, particle concentrations, size distribution, zeta potential, and morphology was reevaluated after 6–12 months of storage at –80 °C. We observed that protein concentration changed only slightly in both pristine and tolvaptan-loaded PDNVs. Particle concentration increased in pristine PDNVs ($5.76 \times 10^{11} \pm 2.24 \times 10^{10}$ particles/mL), while it decreased in tolvaptan-loaded PDNVs sample ($1.82 \times 10^{11} \pm 3.05 \times 10^{10}$ particles/mL) respect to previous measurements. Particle size of pristine (193.0 ± 4.4 nm) and tolvaptan-loaded PDNVs (211.2 ± 30.7 nm) demonstrated a good size stability. Despite slight changes in ζ potential, from −62.45 mV to −55.33 mV in electroporation-prepared PDNVs, and from −51.81 mV to −55.00 mV in pristine PDNVs, all samples maintained comparable surface charge and similar morphology (Figure 2D–F), indicating preserved colloidal and structural stability.

pH-Dependent Drug Release Rate

The release profile of tolvaptan from tomato NVs was analyzed under two pH conditions: physiological (pH 7.4) and slightly acidic (pH 5.0) environments over 48 hours. At pH 7.4, the release rate increased gradually, beginning with an average release of 7% at 1 hour and increasing to 13% at 4 hours, 20% at 24 hours, and 25% by 48 hours (Figure 3). On the other hand, at pH 5.0, the release rate was significantly higher, starting at 12% at 1 hour and rising sharply to 25% at 4 hours, 30% at 24 hours, and finally reaching 39% at 48 hours. The gradual increase in tolvaptan release over time, without an initial burst, indicates a controlled and sustained release mechanism under both physiological and acidic conditions. The results show that release rates vary depending on pH, demonstrating pH-sensitive drug release behavior, with enhanced drug release in acidic environments. This suggests that the nanovesicle system may preferentially release tolvaptan in slightly acidic environments, such as those found in diseased tissues, enhancing its potential for targeted therapeutic applications.

The Effect of Tolvaptan-Loaded Tomato PDNVs on Cytotoxicity and Cell Proliferation

The biological effects of tolvaptan-loaded tomato PDNVs were studied in vitro using different kidney cell lines. Based on previously published data,[20,35] and to avoid toxic doses of PDNVs and tolvaptan, for the cell proliferation and cytotoxicity assays cells were treated with 5 µg of PDNVs (expressed as protein content) in all tests. The tolvaptan-loaded PDNVs contained either 0.25 µg or 2.9 µg tolvaptan to test the dose dependence.

We observed that treatment with tolvaptan alone, especially at higher concentrations, reduced cell proliferation in all cell lines, as indicated by a decrease in the number of cells in phase contrast (Figure 4A).

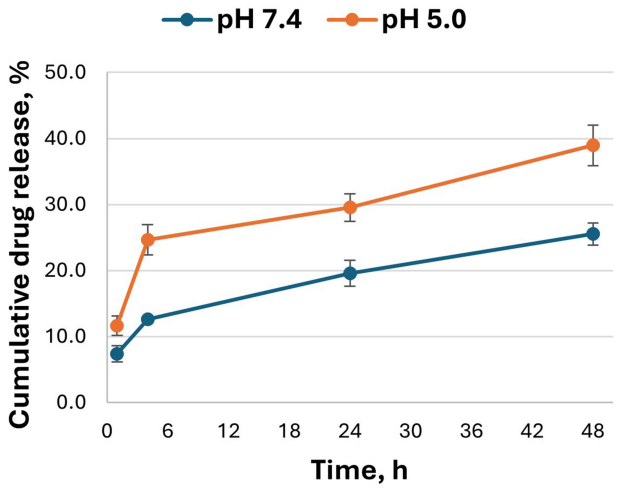

Figure 3 Cumulative drug release profile of tolvaptan-loaded tomato nanovesicles (NVs) at pH 7.4 and pH 5.0 over 48 hours.

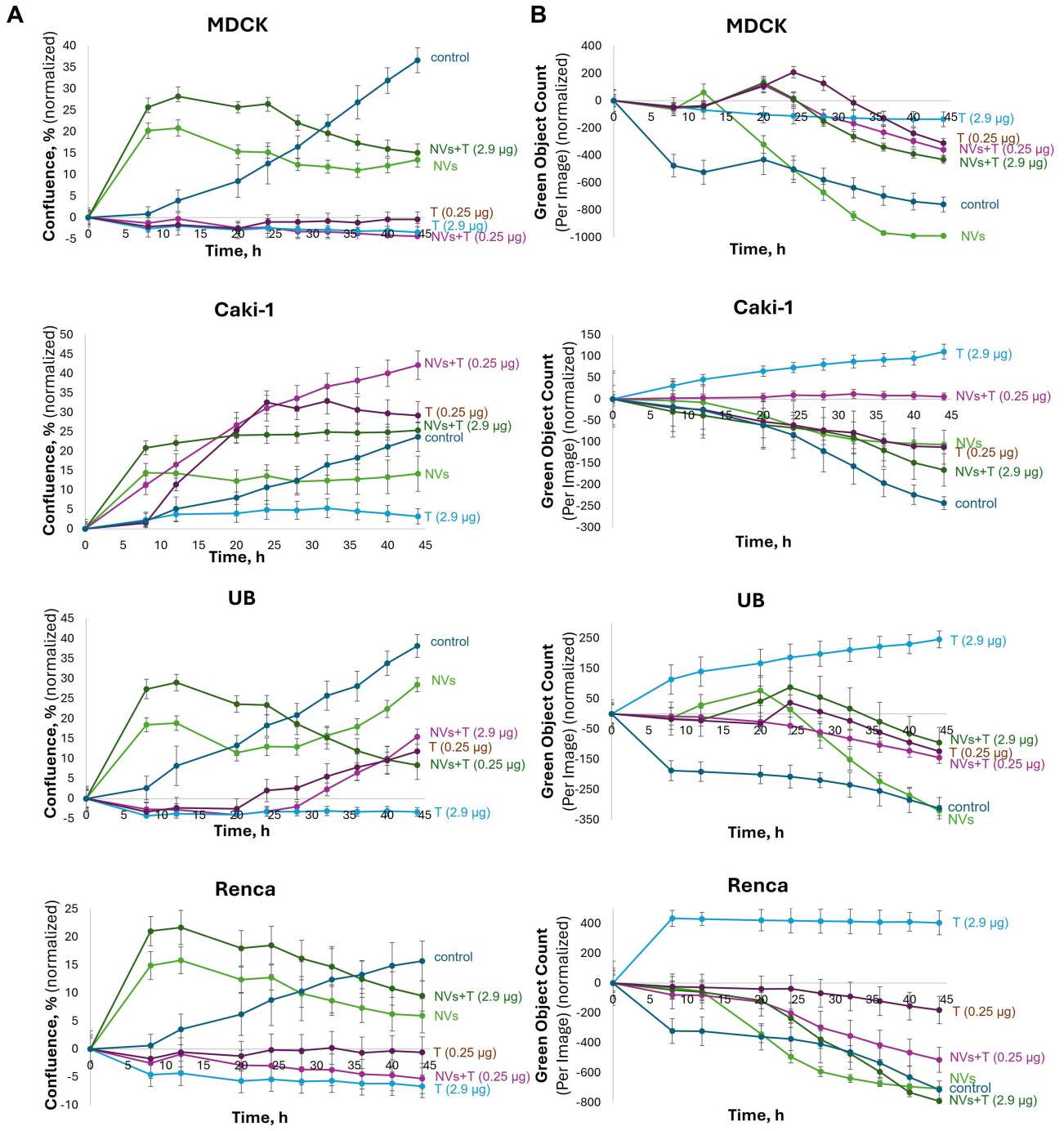

Figure 4 (**A**) Cell proliferation and (**B**) cytotoxicity results of tolvaptan-loaded tomato-derived nanovesicles (NVs) prepared by extrusion and electroporation methods on Caki-1, Madin-Darby canine kidney (MDCK), ureteric bud (UB), and Renca cell lines. Control samples include the same quantity of pristine NVs (5 μg) and tolvaptan (0.25 and 2.9 μg).

In Caki-1 cells, tolvaptan and tolvaptan-loaded PDNVs promoted cell proliferation even at low dose (0.25 μg), whereas pristine PDNVs and tolvaptan at higher dose (2.9 μg) caused moderate increases in confluence. MDCK cells showed a similar pattern, where tolvaptan at both doses and tolvaptan-loaded PDNVs loaded at low dose of tolvaptan resulted in decreased growth of the cells compared to the control sample without any treatment and other samples. This trend continued in UB and Renca cells, showing that treatment with tolvaptan-loaded PDNVs generally surpassed tolvaptan alone in terms of cell proliferation.

https://doi.org/10.2147/IJN.S498012

Additionally, treatment of cells with tolvaptan, particularly at higher doses, led to a significant increase in cell death, as demonstrated by the green fluorescent SYTOX staining (Figure 4B). The treatment of Caki-1 and Renca cell lines with PDNVs and tolvaptan alone enhanced cytotoxicity compared to the treatment using PDNVs loaded with the higher dose (2.9 µg) of tolvaptan. The MDCK cell line followed this trend, with the highest increase in cytotoxicity observed for tolvaptan alone and for tolvaptan-loaded PDNVs. Interestingly, tolvaptan loaded into tomato PDNVs at higher dose were more cytotoxic to the UB cell line than tolvaptan (0.25 µg) alone, pristine PDNVs or low dose tolvaptan-loaded PDNVs. These results, however, collectively suggest that tolvaptan alone at both doses is more toxic to cells, whereas its incorporation into PDNVs reduces its cytotoxicity.

Uptake of Tolvaptan-Loaded Tomato PDNVs by MDCK Cells

To study the uptake of pristine and tolvaptan-loaded tomato PDNVs by the MDCK cell line, cells were treated with $DiOC_{18}$-labelled PDNVs. The cells were stained with nuclear and lysosomal dyes, followed by fixation, and images were captured at 1, 8, and 24 h using a confocal microscope (Figure 5A and B). Figure 5A shows that both pristine and tolvaptan-loaded tomato-derived PDNVs were progressively taken up by cells over time. Clear localization of PDNVs to lysosomes was observed after 24 h of incubation (Figure 5C and D). Slightly more tolvaptan-loaded PDNVs were taken up during the time interval studied. Quantitative colocalization analysis showed similar amounts of unloaded and tolvaptan-loaded PDNVs in lysosomes (Figure 5C and D).

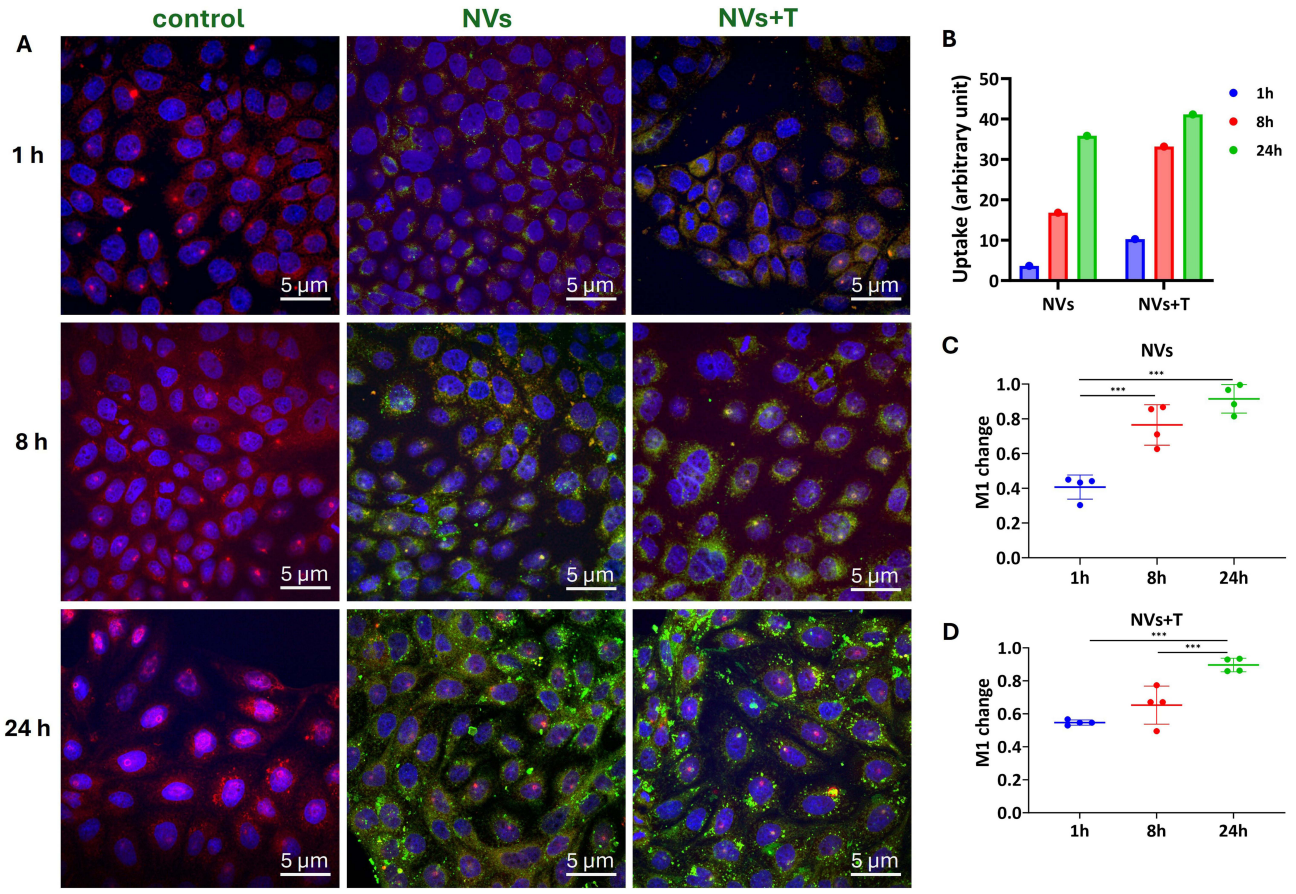

Figure 5 (**A**) Uptake of tomato fruit-derived nanovesicles (NVs) by MDCK cells evaluated by confocal microscopy. $DiOC_{18}$-labelled NVs (green fluorescent) were incubated with cells. (**B**) Cellular uptake of tomato NVs alone (NVs) and with tolvaptan (NVs + T). Cell nuclei were stained with 4′,6-diamidino-2-phenylindole (DAPI) staining (blue), and lysosomes were stained by LysoTracker Deep Red (red); colocalization of (**C**) NVs and (**D**) tolvaptan-loaded NVs (NVs + (**T**) in lysosomes over time; the overlap of the signals is expressed as Manders' M1 coefficient. The level of significance was $p \leq 0.05$ (***).

Quantitative Flow Cytometric Analysis of Tomato PDNVs' Uptake by MDCK Cells

We quantified PDNVs uptake in MDCK cell line using flow cytometry. Figure 6 displays flow cytometry histograms and summary data for time-dependent PDNVs uptake analyzed based on FITC fluorescence (B510-A channel). The control consisted of untreated cells, while experimental groups were cells treated with tolvaptan-loaded PDNV samples for 1, 4, 8, and 24 h). The flow cytometry analysis demonstrated a time-dependent increase both fluorescence intensity of PDNVs and percentage of cell containing PDNVs compared to the control (Figure 6B and C). In the control group, there was a minimal low FITC signal intensity. However, after 1 h there was already an increase in fluorescence intensity and the number of PDNV-containing cells. A sharp increase was observed after 4 and 8 h, and by 24 h uptake of vesicles continued to rise slightly, reaching 55% of cell population and 38,980 counts (Figure 6A and C). Overall, these results confirm that PDNV was efficiently taken up by the cell and in a time-dependent manner.

Application of Tolvaptan-Loaded Tomato PDNVs on Three-Dimensional (3D) MDCK Cell Culture

To study cystogenesis and the effect of tolvaptan-loaded PDNVs on cyst formation and development three-dimensional MDCK cells, an in vitro model of cyst formation, were cultured. After 8 days, cell morphology and cyst formation were monitored using confocal microscopy. Representative images of the cysts are shown in Figure 7A.

Confocal microscopy images revealed major changes in cyst shape across the treatment groups. While the control sample showed a number of circular cysts with well-defined lumens, it was observed that both tolvaptan alone and encapsulated into PDNVs led to a decrease in cyst development and alteration of cyst shape when compared to untreated

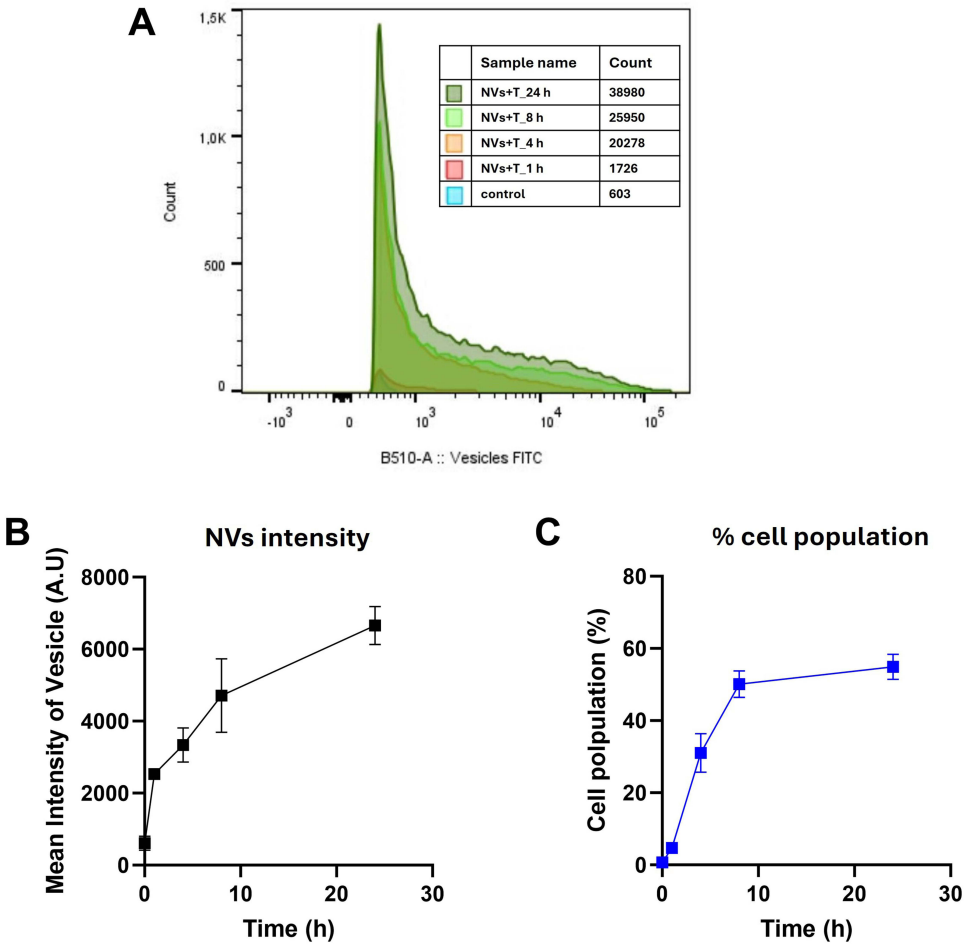

Figure 6 Flow cytometry analysis of uptake tolvaptan-loaded tomato-derived nanovesicles (NVs). (**A**) Histograms showing NVs uptake over time (1, 4, 8, 24 h) compared to untreated control sample. (**B**) Mean intensity of NVs over time. (**C**) Percentage of cell population for NVs uptake over time.

https://doi.org/10.2147/IJN.S498012

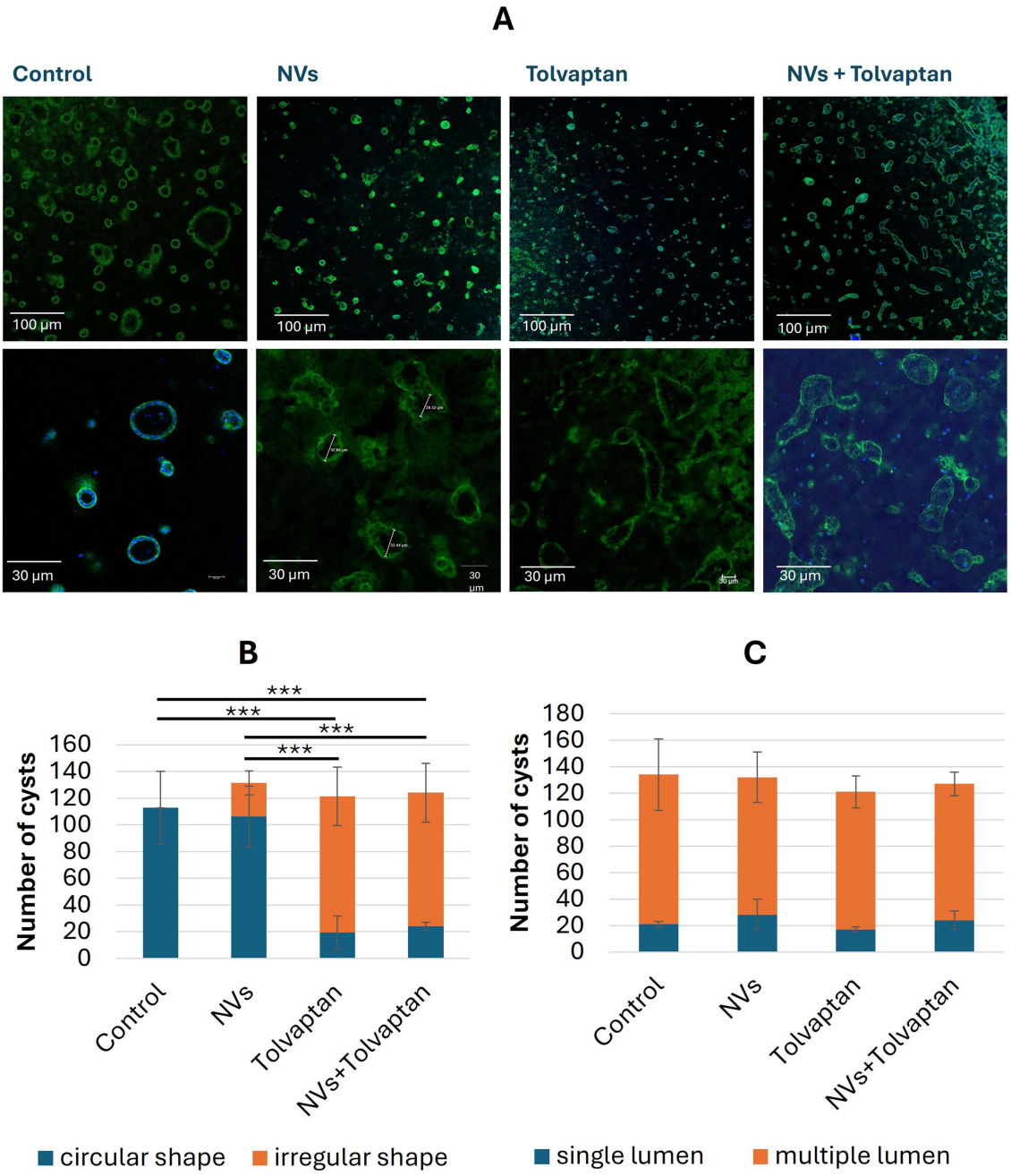

Figure 7 (**A**) Confocal images of cysts formed in three dimensional MDCK cells after 8 days of culture in Matrigel matrix. (**B**) The number of cysts per frame with circular or irregular shape. (**C**) The number of cysts per frame with single or multiple lumens. The level of significance was $p \leq 0.05$ (***).

control sample and pristine tomato PDNVs. Tomato-derived PDNVs treatment reduced the number of cysts with irregular shapes and fewer single lumens. Treatment with tolvaptan, a known inhibitor of cyst growth, resulted in considerable reduction in cyst size and number, with many cysts exhibiting irregular shapes. The morphological deformation of cysts was also monitored when the cells were treated with tolvaptan-loaded tomato PDNVs, with more irregularly shaped cysts indicating a potential synergistic effect of the treatments in suppressing cyst formation.

The number of cysts per frame by the end of day 8 with single or multiple lumens and with circular or irregular shapes is shown in Figure 7B and C. PDNVs, tolvaptan, and tolvaptan-loaded PDNVs showed a significant increase in the number of cysts with irregular shapes ($p \leq 0.05$) compared to the control, which displayed a higher proportion of circular-shaped cysts. Figure 7C shows the number of cysts in single versus multiple lumens. Relatively few single-lumen cysts were observed in all treatment groups, including the control group.

Our results suggest that treatment with native tomato PDNVs, tolvaptan, and tolvaptan-loaded PDNVs altered the morphology of the lumen structure of cysts in MDCK 3D cultures, showing the potential to disrupt cyst growth.

The Effect of Tolvaptan-Loaded Tomato PDNVs on Cell Migration

To quantify the fundamental cell migration characteristics in vitro, an Incucyte ZOOM® 96-well scratch wound migration assay was performed. Caki-1, MDCK, UB, and Renca cells were seeded in 96-well plates and incubated for two days, and the monolayers were scratched using a wound maker. After rinsing the wounds with PBS, serum-free medium containing tomato PDNVs (5 µg), tolvaptan-loaded PDNVs with two different doses of tolvaptan (0.25 and 2.9 µg), and the same quantity of free tolvaptan (0.25 and 2.9 µg) was added to the wells. The rate of gap closure was evaluated using the Incucyte S3 live analysis system for 48 h, and images were obtained using the software every 2 h. The results are shown in Figure 8.

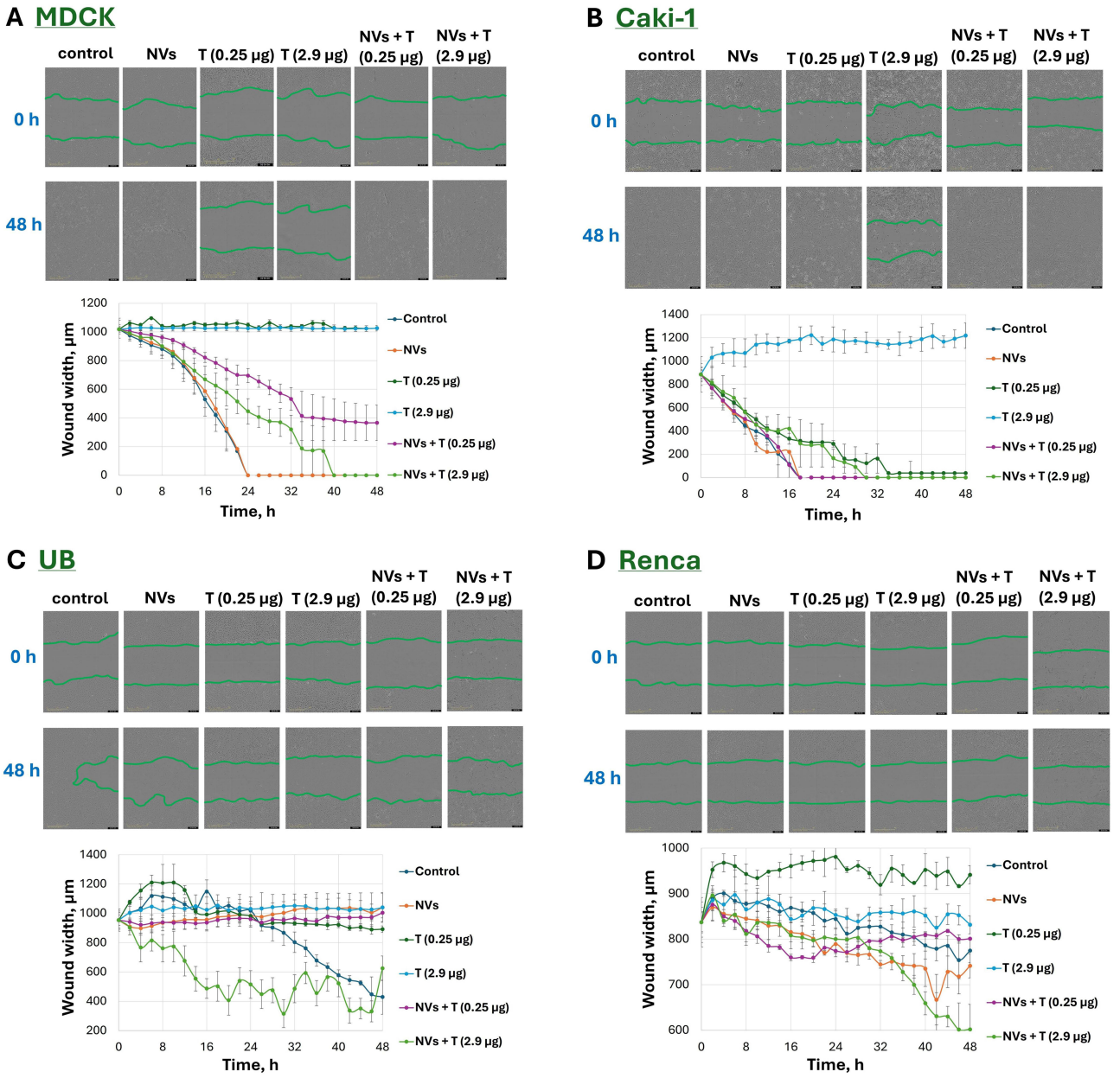

Figure 8 Wound closure was assessed after 48 hours of treatment or without treatment (control sample), wound width measurement and representative images of (**A**) Caki-1, (**B**) MDCK, (**C**) UB, and (**D**) Renca cells (Images were recorded over time using Incucyte S3 live analysis system (EssenBiosciences).

https://doi.org/10.2147/IJN.S498012

Results of scratch wound migration assay performed at various time points demonstrated that treatment with tolvaptan-loaded PDNVs with higher (2.9 μg) and lower (0.25 μg) concentrations leaded the wounds to close entirely after 48 hours on MDCK and Caki-1 cells (Figure 8A and B). However, the improvement in Renca cells was not appreciable (Figure 8D), and on UB cells only the sample treated with a higher dose of tolvaptan was slightly effective (Figure 8C). Nevertheless, all types of cells treated with free drug, especially at higher dose of tolvaptan (2.9 μg), continued to show less progress even after 48 h. A lower dose of free tolvaptan caused the scratch to close completely after 48 h in the Caki-1 cells.

These results indicate that tolvaptan-loaded PDNVs are a more effective delivery system than free tolvaptan, promoting better cell migration and wound closure, particularly in Caki-1 and MDCK cells. Renca and UB cells showed resistance to all treatments, whereas UB cells responded only slightly to tolvaptan-loaded PDNVs with a higher dose of tolvaptan.

Discussion

In our previous work, we showed that native tomato PDNVs inhibit LPS-induced inflammation of THP-1 cells in vitro, and the observed anti-inflammatory effect could be increased by the loading of a natural substance, curcumin.[20] In this study, we aimed to investigate the potential of tomato PDNVs as a nano-drug delivery system for tolvaptan. Tolvaptan is a vasopressin V2 receptor antagonist that has been shown to reduce fluid retention in cysts and slow down the progression of ADPKD.[24,36–38] However, its off-target side effects that significantly affect the patient's quality of life, including hepatotoxicity, excessive urine output, and continuous thirst, remain an issue.[39] Tolvaptan is recognized as a class IV agent of the Biopharmaceutical Classification System and is characterized by both poor solubility and low permeability, which significantly impacts its bioavailability.[21,31,40] Its water solubility is very low, around 50 ng/mL over a pH range of 2–12.[31] Advanced formulation strategies such as solid dispersions, lipid-based delivery systems, and self-microemulsifying drug delivery systems have been introduced with the aim of improving tolvaptan solubility or bioavailability.[31] These methods not only address the solubility challenges but also aim to enhance the overall therapeutic effectiveness of tolvaptan. In this study, we focused on an alternative strategy that leverages the transport capability of PDNVs. Two different loading methods, extrusion and electroporation, were tested and optimized for efficient encapsulation of tolvaptan. The intact vesicular structure of tolvaptan-loaded PDNVs was confirmed by physical (NTA and zeta potential analyses) and morphological (TEM) characterization (Figure 2). The successful cellular uptake of both the pristine and tolvaptan-loaded PDNVs was confirmed using the MDCK model cell line (Figures 5 and 6). In addition, we performed in vitro experiments to evaluate the cytotoxicity and bioactivity of the tolvaptan-loaded tomato fruit-derived PDNVs. Intriguingly, tolvaptan-encapsulated PDNVs showed different cytotoxicity and proliferation in the different cell lines studied (Figure 4A and B). This could be explained by the cell-specific response to tolvaptan, which may be affected by the cellular context and the signaling pathways involved. Generally, low doses of tolvaptan-loaded PDNVs enhanced cell proliferation, suggesting a dose-dependent effect. Moreover, tolvaptan-loaded PDNVs demonstrated less cytotoxicity than tolvaptan alone, thereby demonstrating the potential to improve their therapeutic efficacy in kidney cell models.

Considering that tolvaptan is known as an effective medicine for reducing the weight of the kidney, enlargement of cysts, and progression of ADPKD,[24,36] in this study, we investigated the beneficial effect of tolvaptan-loaded tomato PDNVs on the inhibition of cystic growth by in vitro cyst morphogenesis assay performed on a Matrigel matrix using the MDCK cell line. This cell line is commonly used as a mammalian model of cyst morphogenesis. MDCK cells embedded in the extracellular matrix (eg, collagen and Matrigel) form three-dimensional (3D) cultures, which are spherical cysts with a hollow lumen surrounded by a single layer of polarized cells.[41] These emerging 3D model systems are useful in vitro tools with unique advantages over traditional two-dimensional cell cultures, allowing the study of disease pathways and drug responses. Owing to their ability to better mimic the complex cellular interactions occurring in living organisms, the potential biomedical applications of this approach are broad, including basic biology, clinical research, regenerative medicine, and drug development. We also screened for significant alterations in the cyst morphology after treatment with tolvaptan and tolvaptan-loaded PDNVs. Notably, both tolvaptan alone and when encapsulated in PDNVs resulted in a decrease in cyst size and quantity, as well as an increase in irregularly shaped cysts (Figure 7). The

suppression of cyst growth (Figure 4A) may result from the inhibition of adenylyl cyclase/cyclic AMP pathway, which is known to reduce fluid secretion and cell proliferation.[42]

This finding indicates a possible synergistic effect on cyst growth suppression and a potential therapeutic strategy targeting cystic conditions. As ADPKD has also been reported to potentially increase patient risk for cancer, further investigation of shared targets between ADPKD and cancer could assist in identifying shared susceptibility to both diseases and the development of preventative therapeutic measures. The results of the Incucyte ZOOM® scratch wound migration assay demonstrated that tolvaptan-loaded tomato PDNVs at two different doses had a relatively favorable effect on enhancing wound healing and cell migration in mammalian kidney cell models, particularly in Caki-1 and MDCK cells (Figure 8).

In contrast, UB and Renca cells showed resistance to all treatments, suggesting the need for further investigation into the mechanisms underlying their reduced responsiveness.

Overall, in this study, we demonstrated that tomato PDNVs have potential as next-generation targeted nanodelivery systems by encapsulating a synthetic hydrophobic drug used in the treatment of ADPKD and other kidney disorders. However, further studies are needed to improve the drug-loading capacity and to reveal the underlying mechanisms of action. Furthermore, in vivo experiments are necessary to evaluate the therapeutic efficacy of tolvaptan-loaded PDNVs in kidney-related conditions.

Conclusion

In this study, we explored the use of PDNVs as an effective nanodelivery system for a synthetic drug, a vasopressin V2-receptor antagonist used in the treatment of ADPKD. By comparing the two loading methods, electroporation and extrusion – electroporation showed better efficiency for drug loading.

Cytotoxicity assays revealed that tolvaptan-loaded PDNVs had varying effects on the viability of different renal cell lines, with some showing enhanced proliferation. Additionally, tolvaptan-loaded PDNVs were effectively taken up by MDCK cells, and a cyst formation assay using MDCK cells confirmed that tolvaptan-loaded PDNVs inhibited cyst formation and altered the cyst shape, underscoring their therapeutic potential in polycystic kidney disease. These PDNVs also showed promise in enhancing cell migration, particularly in Caki-1 and MDCK cell lines.

Overall, tomato-derived PDNVs show promise as a natural next-generation nanoscale delivery system capable of improving the therapeutic efficacy of hydrophobic drugs, such as tolvaptan. Future in vivo studies are necessary to validate the therapeutic potential of tolvaptan-loaded PDNVs and to further optimize the drug-loading process.

Acknowledgments

This project received funding from the European Union's Horizon 2020 Research and Innovation Programme under the Marie Skłodowska-Curie Staff Exchange project "FarmEVs", grant agreement N. 101131175. The views and opinions expressed in this publication are solely those of the authors and do not necessarily reflect those of the European Union. Neither the European Union nor the granting authority can be held responsible. The authors would like to acknowledge Carmen Laezza and Giovanna Schiavone seconded staff members of FarmEVs project for their contributions to this work.

Ramila Mammadova gratefully acknowledges the support from the Erasmus and EDUFI grants for facilitating short-term training at the University of Oulu and the support from the Jenny and Antti Wihuri Foundation for her postdoctoral fellowship.

The authors acknowledge the contribution of the Biocenter Oulu Light Microscopy Core Facility, part of Biocenter Finland's biological imaging platform, and the help of Veli-Pekka Ronkainen in the acquisition of confocal images. We acknowledge the University of Oulu Mining School for their support in zeta potential measurements. We are very grateful to Irina Raykhel for her advice on the cystogenesis experiments. Special thanks go to Johanna Kekolahti-Liias and Paula Haipus for their technical assistance.

Disclosure

The authors report no conflicts of interest in this work.

References

1. Gao J, Karp JM, Langer R, Joshi N. The future of drug delivery. *Chem Mater*. 2023;35(2):359. doi:10.1021/ACS.CHEMMATER.2C03003
2. Du S, Guan Y, Xie A, et al. Extracellular vesicles: a rising star for therapeutics and drug delivery. *J Nanobiotechnology*. 2023;21(1):1–51. doi:10.1186/S12951-023-01973-5
3. Yang C, Zhang W, Bai M, et al. Edible plant-derived extracellular vesicles serve as promising therapeutic systems. *Nano Trans Med*. 2023;2 (2–3):100004. doi:10.1016/J.NTM.2023.100004
4. Alzahrani FA, Khan MI, Kameli N, Alsahafi E, Riza YM. Plant-derived extracellular vesicles and their exciting potential as the future of next-generation drug delivery. *Biomolecules*. 2023;13(5):839. doi:10.3390/BIOM13050839
5. Fang Z, Liu K. Plant-derived extracellular vesicles as oral drug delivery carriers. *J Control Release*. 2022;350:389–400. doi:10.1016/J.JCONREL.2022.08.046
6. Abraham AM, Wiemann S, Ambreen G, et al. Cucumber-derived exosome-like vesicles and plantcrystals for improved dermal drug delivery. *Pharmaceutics*. 2022;14(3):476. doi:10.3390/PHARMACEUTICS14030476
7. Man F, Meng C, Liu Y, et al. The study of ginger-derived extracellular vesicles as a natural nanoscale drug carrier and their intestinal absorption in rats. *AAPS Pharm Sci Tech*. 2021;22(6). doi:10.1208/S12249-021-02087-7
8. Mao Y, Han M, Chen C, et al. A biomimetic nanocomposite made of a ginger-derived exosome and an inorganic framework for high-performance delivery of oral antibodies. *Nanoscale*. 2021;13(47):20157–20169. doi:10.1039/D1NR06015E
9. Zhang M, Xiao B, Wang H, et al. Edible ginger-derived nano-lipids loaded with doxorubicin as a novel drug-delivery approach for colon cancer therapy. *Mol Ther*. 2016;24(10):1783–1796. doi:10.1038/mt.2016.159
10. Zhang M, Wang X, Han MK, Collins JF, Merlin D. Oral administration of ginger-derived nanolipids loaded with siRNA as a novel approach for efficient siRNA drug delivery to treat ulcerative colitis. *Nanomedicine*. 2017;12(16):1927–1943. doi:10.2217/NNM-2017-0196
11. Wang Q, Ren Y, Mu J, et al. Grapefruit-derived nanovectors use an activated leukocyte trafficking pathway to deliver therapeutic agents to inflammatory tumor sites. *Cancer Res*. 2015;75(12):2520–2529. doi:10.1158/0008-5472.CAN-14-3095
12. Zhuang X, Teng Y, Samykutty A, et al. Grapefruit-derived nanovectors delivering therapeutic miR17 through an intranasal route inhibit brain tumor progression. *Mol Ther*. 2016;24(1):96–105. doi:10.1038/MT.2015.188
13. Teng Y, Mu J, Hu X, et al. Grapefruit-derived nanovectors deliver miR-18a for treatment of liver metastasis of colon cancer by induction of M1 macrophages. *Oncotarget*. 2016;7(18):25683–25697. doi:10.18632/ONCOTARGET.8361
14. Fang Z, Song M, Lai K, Cui M, Yin M, Liu K. Kiwi-derived extracellular vesicles for oral delivery of sorafenib. *Eur J Pharm Sci*. 2023;191:106604. doi:10.1016/J.EJPS.2023.106604
15. You JY, Kang SJ, Rhee WJ. Isolation of cabbage exosome-like nanovesicles and investigation of their biological activities in human cells. *Bioact Mater*. 2021;6(12):4321–4332. doi:10.1016/j.bioactmat.2021.04.023
16. Zhang L, He F, Gao L, et al. Engineering exosome-like nanovesicles derived from asparagus cochinchinensis can inhibit the proliferation of hepatocellular carcinoma cells with better safety profile. *Int J Nanomed*. 2021;16:1575–1586. doi:10.2147/IJN.S293067
17. Bokka R, Ramos AP, Fiume I, et al. Biomanufacturing of tomato-derived nanovesicles. *Foods*. 2020;9(12):1852. doi:10.3390/foods9121852
18. Nemati M, Singh B, Mir RA, et al. Plant-derived extracellular vesicles: a novel nanomedicine approach with advantages and challenges. *Cell Commun Signal*. 2022;20(1):1–16. doi:10.1186/S12964-022-00889-1
19. Mammadova R, Fiume I, Bokka R, et al. Identification of tomato infecting viruses that co-isolate with nanovesicles using a combined proteomics and electron-microscopic approach. *Nanomaterials*. 2021;11(8):1922. doi:10.3390/nano11081922
20. Mammadova R, Maggio S, Fiume I, et al. Protein biocargo and anti-inflammatory effect of tomato fruit-derived nanovesicles separated by density gradient ultracentrifugation and loaded with curcumin. *Pharmaceutics*. 2023;15(2):333. doi:10.3390/pharmaceutics15020333
21. Schrier RW, Gross P, Gheorghiade M, et al. Tolvaptan, a selective oral vasopressin V2-receptor antagonist, for hyponatremia. *N Engl J Med*. 2006;355(20):2099–2112. doi:10.1056/NEJMOA065181
22. Prosperi F, Suzumoto Y, Marzuillo P, et al. Characterization of five novel vasopressin V2 receptor mutants causing nephrogenic diabetes insipidus reveals a role of tolvaptan for M272R-V2R mutation. *Sci Rep*. 2020;10(1):1–11. doi:10.1038/s41598-020-73089-x
23. Yi JH, Shin HJ, Kim HJ. V2 Receptor Antagonist; Tolvaptan. *Electrolytes Blood Press E BP*. 2011;9(2):50. doi:10.5049/EBP.2011.9.2.50
24. Torres VE, Chapman AB, Devuyst O, et al. Tolvaptan in patients with autosomal dominant polycystic kidney disease. *N Engl J Med*. 2012;367 (25):2407. doi:10.1056/NEJMOA1205511
25. Torres VE, Meijer E, Bae KT, et al. Rationale and design of the TEMPO (tolvaptan efficacy and safety in management of autosomal dominant polycystic kidney disease and its outcomes) 3-4 study. *Am J Kidney Dis*. 2011;57(5):692–699. doi:10.1053/J.AJKD.2010.11.029
26. Van Gastel MDA, Torres VE. Polycystic kidney disease and the vasopressin pathway. *Ann Nutr Metab*. 2017;70(Suppl. 1):43–50. doi:10.1159/000463063
27. Sinha S, Dwivedi N, Tao S, et al. Targeting the vasopressin type-2 receptor for renal cell carcinoma therapy. *Oncogene*. 2019;39(6):1231–1245. doi:10.1038/s41388-019-1059-0
28. Torres VE, Chapman AB, Devuyst O, et al. Tolvaptan in later-stage autosomal dominant polycystic kidney disease. *N Engl J Med*. 2017;377 (20):1930–1942. doi:10.1056/NEJMOA1710030
29. Kim Y, Han S. Recent updates in therapeutic approach using tolvaptan for autosomal dominant polycystic kidney disease. *Korean J Intern Med*. 2023;38(3):322–331. doi:10.3904/KJIM.2022.376
30. Li T, Li GS. Hypernatremia induced by low-dose Tolvaptan in a Patient with refractory heart failure: a case report. *Medicine*. 2019;98(27). doi:10.1097/MD.0000000000016229
31. Lee JH, Lee GW. Formulation approaches for improving the dissolution behavior and bioavailability of tolvaptan using SMEDDS. *Pharmaceutics*. 2022;14(2). doi:10.3390/PHARMACEUTICS14020415
32. Fujiki H, Matsunaga M, Furukawa M, et al. In vitro and in vivo pharmacological profile of OPC-61815, a water-soluble phosphate ester pro-drug of tolvaptan. *J Pharmacol Sci*. 2022;150(3):163–172. doi:10.1016/J.JPHS.2022.08.004
33. Barasch J, Pressler L, Connor J, Malik A. A ureteric bud cell line induces nephrogenesis in two steps by two distinct signals. *Am J Physiol*. 1996;271(1 PART 2):F50–61. doi:10.1152/AJPRENAL.1996.271.1.F50
34. Scientific Image and Illustration Software | BioRender. Available from: https://www.biorender.com/. Accessed January 24, 2024.

35. Tunçdemir BE. Can tolvaptan usage cause cytotoxicity? An in vitro study. *Eur Res J*. 2023;9(3):454–460. doi:10.18621/eurj.1058030
36. Kim HY, Lee SJ, Kim BK, et al. Long-term Tolvaptan Treatment of Autosomal Dominant Polycystic Kidney Disease in Korea. *Electrolytes Blood Press E BP*. 2018;16(2):23. doi:10.5049/EBP.2018.16.2.23
37. Dixon MB, Lien YH. Tolvaptan and its potential in the treatment of hyponatremia. *Ther Clin Risk Manag*. 2008;4(6):1149. doi:10.2147/TCRM.S3115
38. Al Therwani S, Malmberg MES, Rosenbaek JB, Bech JN, Pedersen EB. Effect of tolvaptan on renal handling of water and sodium, GFR and central hemodynamics in autosomal dominant polycystic kidney disease during inhibition of the nitric oxide system: a randomized, placebo-controlled, double blind, crossover study. *BMC Nephrol*. 2017;18(1):1–13. doi:10.1186/S12882-017-0686-3/TABLES/6
39. Blair HA. Tolvaptan: a review in autosomal dominant polycystic kidney disease. *Drugs*. 2019;79(3):303–313. doi:10.1007/S40265-019-1056-1/METRICS
40. Goods administration T. Australian public assessment report for tolvaptan; 2018. Available from: https://www.tga.gov.au. Accessed August 31, 2024.
41. Elia N, Lippincott-Schwartz J. Culturing three dimensional MDCK cells for analyzing intracellular dynamics. *Curr Protoc Cell Biol*. 2009;43. doi:10.1002/0471143030.CB0422S43
42. Zhou X, Torres VE. Emerging therapies for autosomal dominant polycystic kidney disease with a focus on cAMP signaling. *Front Mol Biosci*. 2022;9:981963. doi:10.3389/FMOLB.2022.981963